Use of Complex Source Beam-Moment Method for Solving Scattering Problems from Terrain Profiles

Alexandre Alves da Rocha
PPGEE, Postgraduate Program in Electrical Engineering
Federal University of Minas Gerais
Av. Antonio Carlos 6627, 31270-901
Belo Horizonte, MG, Brazil
Email: alexandrear@ufmg.br

Cássio G. Rego*, Fernando J.S. Moreira§
* §DELT, Departament of Electronic Engineering
Federal University of Minas Gerais
Av. Antonio Carlos 6627, 31270-901
Belo Horizonte, MG, Brazil
Email: *cassio@cpdee.ufmg.br, §fernandomoreira@ufmg.br

***Abstract*—This work presents results involving the application of the CSB-MoM, a new hybrid complex source beam moment method, as an algorithm that analyzes propagation and scattering problems over large terrains. Thus, the formulation of the CSB-MoM is presented and then applied to a two-dimensional terrain profile. It is shown that the method can successfully reduce the memory and storage requirements, as well as average CPU time to a scale of $O(N^{3/2})$ as opposed to O(N^2) of the standard MoM.**

I. Introduction

The CSB-MoM is a hybrid method that combines the MoM with the CSB expansion technique [1] in the solution of large electromagnetic problems. Its purpose is to accelerate the matirx-vector product (MVP) from the iterative solutions of the standard MoM problems related to this kind of geometries. In the CSB-MoM, the CSBs are not the basis functions for the MoM. Instead, they are used to expand the fields of basis functions to make a faster evaluation of field interactions between the groups in the iterative solutions. The right choice of group sizes in which the basis elements are combined into M groups leads the operational count of the MVP and the storage requirement to be lessened to $O(N^{3/2})$, for both memory and computational time as opposed to the standard MVP. It is important to note that this procedure can be applied to both homogeneous and inhomogeneous space problems since it can take on any form of the Green's functions.

The CSB-MoM algorithm [2], [3] share similarities with the Fast Multipole Method (FMM). In both approaches the subsectional basis elements defined on the object surface are grouped (Fig. 2) and the interactions for the neighboring and self groups happen in the standard way. However, for the interactions of the well separated groups, the fields of the basis functions are expanded in terms of CSBs, once they are exact solutions of Maxwell's equations [1], [2], [4], [5]. To compute the interactions between the well separated groups, their equivalent CSB expansions are interacted utilizing only a small portion of the CSBs from each group, due to the CBSs's natural Gaussian like windowing property. Because of that, the matrices generated by this method become highly sparse [6], which provides a better efficiency to the computation of the well separated group interactions. However, an important difference between CSB-MoM and the FMM is that the latter generates a diagonal translation operator for separated pairs of groups, while the CSB-MoM produces a very sparse translation operator.

Thus, this work proposes an analysis of the potential of the CSB-MoM algorithm in the solution of large EM problems on a terrain profile. To achieve this goal, the present study is structured as follows: we first present the Problem Formulation on Section II, where the terrain profile is characterized. Next, on Section III, the CSB-MoM approach is discussed in more detail, including the Standard CSB-MoM formulation, the Formation of Groups, the formation of CSP Beam for the Groups, and the CSB-MoM Group Interactions. Section IV shows the numerical results achieved. Finally, Section V is dedicated to the conclusion of what has been discussed here.

II. Problem Formulation

The problem consists in the prediction of the electromagnetic field intensity in any point in space when an irregular terrain is illuminated by a transmission source. The terrain is considered to be invariant in the direction perpendicular to the propagation direction in order to reduce two-dimension (2D) problem analysis.The terrain profile along the axis x is characterized by curve C defined by $z = f(x)$, as shown in Fig. 1. In this paper, the terrain is considered an imperfect and inhomogeneous conductor modeled by a superficial impedance s and the ground losses are approximated by Leontovich boundary conditions [7].

As demonstrated in [8], the incident electromagnetic field is divided into transverse magnetic polarization (TM_y) in respect to the coordinate y (or horizontal polarization), defined by $E^{inc}(\boldsymbol{\rho}) = E_y^{inc}(\boldsymbol{\rho})$, being the EFIE expressed by

$$-E_y^{inc}(\boldsymbol{\rho}) = -\eta_s J_y(\boldsymbol{\rho}) - j\omega_0\mu_0 \int_C J_y(\boldsymbol{\rho'}) G(\boldsymbol{\rho}, \boldsymbol{\rho'}) d\rho' + \int_C \eta_s J_y(\boldsymbol{\rho'}) \left[\hat{n}' \cdot \nabla G(\boldsymbol{\rho}, \boldsymbol{\rho'})\right] d\rho', \quad (1)$$

and transverse electric polarization (TE_y) (or vertical polarization), established by $H^{inc}(\boldsymbol{\rho}) = H_y^{inc}(\boldsymbol{\rho})$, being the MFIE

978-1-4673-9492-5/15/$31.00 ©2015 IEEE

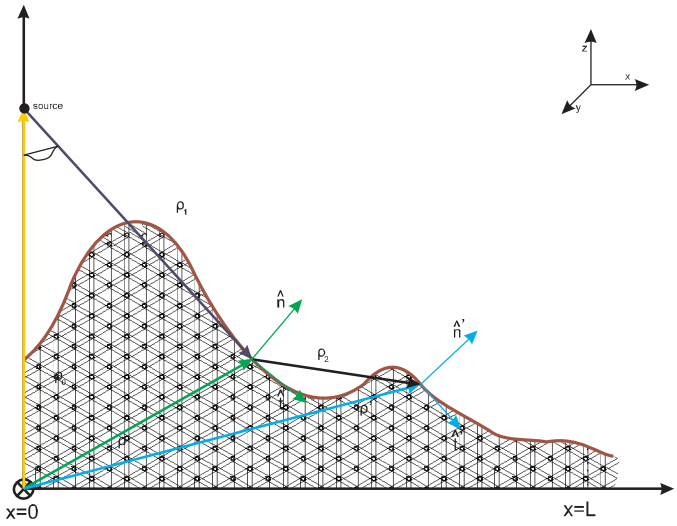

Fig. 1. The Problem Geometry / Representation of the vectors in the problem analysis.

expressed by

$$-H_y^{inc}(\boldsymbol{\rho}) = J_t(\boldsymbol{\rho}) - \int_C J_t(\boldsymbol{\rho}')\left[\hat{n}'\cdot\nabla G(\boldsymbol{\rho},\boldsymbol{\rho}')\right]d\rho' + j\omega_0\epsilon_0\int_C \eta_s J_t(\boldsymbol{\rho}')G(\boldsymbol{\rho},\boldsymbol{\rho}')d\rho', \quad (2)$$

where $G(\boldsymbol{\rho},\boldsymbol{\rho}') = -(j/4)H_o^2(k_0\,|\boldsymbol{\rho}-\boldsymbol{\rho}'|)$ is the two-dimension Green's function for the free space, k_0 is the air wave number $\hat{n}'$ is the normal unit vector to the surface on the point localized by the vector $\boldsymbol{\rho}'$, and μ_0, ϵ_0 are the air magnetic permeability and electric permissibility respectively.

III. The CSB-MoM Approach

A. The Standard MoM Formulation

In the conventional MoM procedure the terrain profile in Fig. 1 is first represented by N line segments. The next step is the application of similar numerical technique procedures to solve the EFIE and the MFIE to the unknown electric current density $\mathbf{J}(\boldsymbol{\rho}')$. Then $\mathbf{J}(\boldsymbol{\rho}')$ is expanded into a finite series in the form of

$$\mathbf{J}(\boldsymbol{\rho}') = \sum_{n=1}^{N} I_n \mathbf{f}_n(\boldsymbol{\rho}'). \quad (3)$$

In the adopted notation $(\rho, \hat{\eta}, \hat{t})$ is associated to the observation point in segment i, and $(\rho', \hat{\eta}', \hat{t}')$ is associated to the source point in segment j. Next, the integral equations (1) and (2) are discretized into a system of linear equations. In addition, point-matching with pulse basis functions is applied, resulting in a matrix equation

$$[\mathbf{V}] = [\bar{\boldsymbol{Z}}][\bar{\boldsymbol{I}}], \quad (4)$$

where $[\bar{\boldsymbol{Z}}]$ is the MoM impedance matrix of dimension $(N \times N)$, N is the number of unknowns, $[\mathbf{V}]$ is the excitation vector of dimension $(N \times 1)$ whose incident fields are evaluated at the matching points, and $[\bar{\boldsymbol{I}}]$ corresponds to the solution vector containing the unknown current coefficients. The elements of the impedance matrix to the EFIE and the MFIE are formed respectively by

$$Z_{nn'}^{(E)} = -\int_{S_n}\int_{S_{n'}} \mathbf{f}_n(\boldsymbol{\rho})\cdot\bar{\bar{G}}(\boldsymbol{\rho}|\boldsymbol{\rho}')\cdot\mathbf{f}_{n'}(\boldsymbol{\rho}')d\rho' d\rho, \quad (5)$$

$$Z_{nn'}^{(H)} = -\int_{L_n}\int_{L_{n'}} \mathbf{g}_n(\boldsymbol{\rho})\cdot\bar{\bar{G}}_{me}(\boldsymbol{\rho}|\boldsymbol{\rho}')\cdot\mathbf{f}_{n'}(\boldsymbol{\rho}')d\rho' d\rho, \quad (6)$$

where S_n is in the local support of testing functions $\mathbf{f}_n$, L_n is in the local support of testing functions $\mathbf{g}_n$; $L_{n'}$ is in the local support of $\mathbf{f}_{n'}$ and the dyadic Green's function $\bar{\bar{G}}_{me}$ for the magnetic field of an electric current $\bar{\bar{G}}_{me}(\boldsymbol{\rho},\boldsymbol{\rho}') = (1/4\pi)\nabla G_0(\boldsymbol{\rho},\boldsymbol{\rho}')\times\bar{\bar{I}}$, and $G_0(\boldsymbol{\rho},\boldsymbol{\rho}') = e^{-jkR}/R$ and $\bar{\bar{I}}$ denotes the identity dyad. For convenience, the indexes E and H will be adopted to relate to the EFIE and MFIE fields respectively.

B. Group Formation

The groups are formed after the definition of the basis function subsections on the terrain surface, so that M groups of similar size enclosure N/M profile segments. Fig. 2 shows the formation these and the distribution of these segments. In order to guarantee the correspondence between the groups formed and the the localization of the basis function subsections on the profile, a global index $n \longleftrightarrow (m,i)$ is defined, where $i = 1, 2, 3, ..., N/M$. Therefore, the correspondece between the pairs of groups and the conventional MoM impedance matrix Z subblocks is assured. It is important to note that the diameter of the CSBs expansion circle keeps a direct relation with the group formation, once it is chosen in a way that it completely surrounds the group.

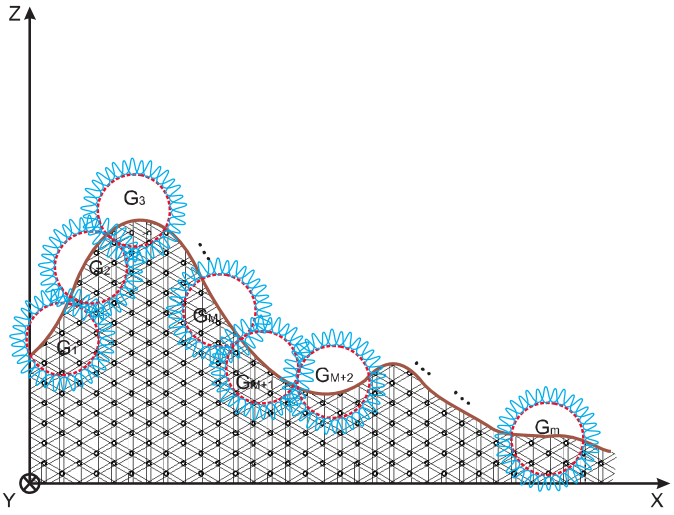

Fig. 2. The problem and its M groups, each enclosing N/M elements.

C. Formation Of CSBs for the Groups

The definition of the CSBs is performed after the group formation, adopting the CSB expansion method, with electric

equivalent current $\mathbf{J}_{eq}$ only [1]. The equivalent representation to the case proposed in this work can be expressed for EFIE by

$$\boldsymbol{E}_{mi}^{(E)}(\boldsymbol{\rho}) = \int_{o}^{2\pi} \bar{\bar{G}}(\boldsymbol{\rho}|\tilde{\boldsymbol{\rho}}'_{\boldsymbol{mq}})\tilde{\mathbf{J}}_{\mathbf{eq}}(\tilde{\boldsymbol{\rho}}')\tilde{a}d\phi', \tag{7}$$

where $\tilde{\boldsymbol{\rho}}' = \tilde{a}\hat{p}'$, being $\hat{p}' = \hat{x}cos\phi' + \hat{y}sin\phi'$. For simplicity, (7) is discretized, originating

$$\boldsymbol{E}_{mi}^{(E)}(\boldsymbol{\rho}) = \sum_{q=1}^{Q} \bar{\bar{G}}(\boldsymbol{\rho}|\tilde{\boldsymbol{\rho}}'_{\boldsymbol{mq}})\mathbf{w}_{miq}, \tag{8}$$

and it is next analyzed on a test surface, where Q is the total number of beams in the discretized expansion, $\mathbf{w}_{miq}$ represents the unknown weight functions to be solved, $\tilde{\boldsymbol{\rho}}'_{\boldsymbol{miq}}$ denotes the complex localizations for the font $\mathbf{J}_{eq}$, and $\tilde{a} = D_g/2 - jb_0$. A detailed study on the definitions of b_0 and Q is found in [2]. The Green's function with complex source arguments generates CSP beams [1], [9]. It is noted that the complex locations of the complex sources $\tilde{\boldsymbol{\rho}}'_{\boldsymbol{mq}}$ are the same for all elements in the group and they measured relatively to the global coordinate system centered at the origin. The summation in. (8) is obtained by numerically integrating Eq. (7) with sampling at the points $\tilde{\boldsymbol{\rho}}'_{\boldsymbol{mq}}$ [3].

Similar procedures must be adopted in order to establish the unknown vector beam weights to the MFIE $\mathbf{u}_{miq}$, so as to produce

$$\boldsymbol{E}_{mi}^{(H)}(\boldsymbol{\rho}) = \sum_{q=1}^{Q} \bar{\bar{G}}_{me}(\boldsymbol{\rho}|\tilde{\boldsymbol{\rho}}'_{\boldsymbol{mq}})\mathbf{u}_{miq}. \tag{9}$$

D. CSB-MoM Group Interactions

The CSB-MoM hybrid algorithm is a process that works with highly sparse matrices. This process is implemented by decomposing the matrix, according to

$$[\boldsymbol{Z}] = [\boldsymbol{Z}'] + [\mathbf{U}]^{\mathbf{T}}[\mathbf{T}][\mathbf{U}]. \tag{10}$$

Such decomposition can be analyzed in two steps. The first one corresponds to the interaction between the near groups, represented in (10) by $[\boldsymbol{Z}']$, defined by the standard MoM procedure, and differing from it for generating a highly sparse martrix. The second step deals with the interactions between the far groups, which must be analyzed by $[\mathbf{U}]^{\mathbf{T}}[\mathbf{T}][\mathbf{U}]$, where U is composed by the CSP beams coefficients and T is the reaction between the beams associated with the well separated groups. It is important to note that the near group definition is dependent on the distance between the center of the two groups. Therefore, the critical distance D_{near} is first defined, completely depends on the expansion circle complex radius as well as the established threshold error ϵ_t, presented in more detail in [2]. For the case of the 2D problem proposed, it must be $D_{near} = 2\,|\tilde{a}| = 2\sqrt{a^2 + b^2}$. Thus, the near groups are located in a distance that is inferior to D_{near}.

1) Near/Self: As already mentioned, two groups are considered near when their critical distance is inferior to D_{near}. This way, we have adjacent groups whose basis elements subsection interaction is developed through the conventional MoM. IN other words, they must be calculated using the auto impedance term $Z_{nn'}$ oriented by the global index in (5). It is possible to observe that the structure of $[\boldsymbol{Z}']$ is a matrix $(M \times M)$, generally sparse and not structured, so that only the non zero blocks must be stored to reduce the allocated space in memory.

2) CSBs: Resorting to the CSB expansion it is possible to calculate the mutual impedance between the $Z_{nn'}$ elements, oriented by the global index in (5), replacing the second integral by the representaiTion through the CSBs (10), changing the the order of both the sum and the integration with the use of reciprocity properties and symmetries of dyatic Green's functions, and the field integration of $\mathbf{f}_n$ evaluated in the complex localization of $G_{m'}$. Thus, we have its representation in [6] by

$$Z_{nn'}^{(E)} = -\sum_{q=1}^{Q}\sum_{q'=1}^{Q} \mathbf{w}_{miq}\bar{\bar{G}}(\boldsymbol{\rho}|\tilde{\boldsymbol{\rho}}')\mathbf{w}_{m'i'q'}, \tag{11}$$

$$Z_{nn'}^{(H)} = -\sum_{q=1}^{Q}\sum_{q'=1}^{Q} \mathbf{u}_{miq}\bar{\bar{G}}(\boldsymbol{\rho}|\tilde{\boldsymbol{\rho}}')\mathbf{w}_{m'i'q'}. \tag{12}$$

The (11) and the (12) are closely related to the terms $[\mathbf{U}]^{\mathbf{T}}[\mathbf{T}][\mathbf{U}]$ and can be rewritten, for simplicity, according to (13) and (14) respectively. Due to the complex argument analytical properties in G, only a small portion of the CSBs in this double sum contribute significantly to $Z_{nn'}$ because of the CSBs natural windowing properties [1]. Another advantage of the method is thus noticed, once a full matrix of dimension $(Q \times Q)$ becames highly sparse.

$$[\boldsymbol{Z}_{\boldsymbol{mm'}}^{(\boldsymbol{E})}] = [\mathbf{U_m}]^{\mathbf{T}}[\mathbf{T_{mm'}}][\mathbf{U_{m'}}], \tag{13}$$

$$[\boldsymbol{Z}_{\boldsymbol{mm'}}^{(\boldsymbol{H})}] = [\mathbf{Y_m}]^{\mathbf{T}}[\mathbf{T_{mm'}}][\mathbf{U_{m'}}]. \tag{14}$$

Note that once the elements of $[\mathbf{U_{m'}}]$, where $[\mathbf{U'_m}]$ is $\mathbf{w}_{m'i'q'}$ and $[\mathbf{Y_{m'}}]$, where $[\mathbf{Y'_m}]$ is $\mathbf{u}_{m'i'q'}$, respectively in (8) and (9), are calculated, they are stored to be used in future interactions, as in (13) and (14), reducing, therefore, the computational cost in this process. In possession of such information, we have all the necessary elements to develop the calculation of (10).

IV. Numerical Results

The numerical results obtained indicate that the algorithm proposed by [6] has a highly relevant potential to the solution of large scale EM problems, as well as to the analysis of topographical profiles. The interactions between the groups of the expansion G_m e $G_{m'}$ evaluated through the CSB-MoM, namely, $T_{mm'}$ are shown in Fig. 3. These correspond to the interactions of the well separated groups according to the critical distance established by D_{near} and the conditions of the circle complex radius $\tilde{a}$. Note that the region with significant

elements, that is, magnitudes superior to $-140dB$, is a small region in the graphic, represented by the hot colors. However, the position of the hot colors may suffer changes according to the problem geometry and to the location of the groups of the expansion G_m e $G_{m'}$. The remaining elements can be neglected in this technique. It is important to stress that these interactions are valid only for well separated groups because if the evaluation occurred to neighbouring groups (groups whose center to center distance is inferior to D_{near}), the technique would have its accuracy impaired due to the overlapping of the CSBs branch cuts radiated by two groups.

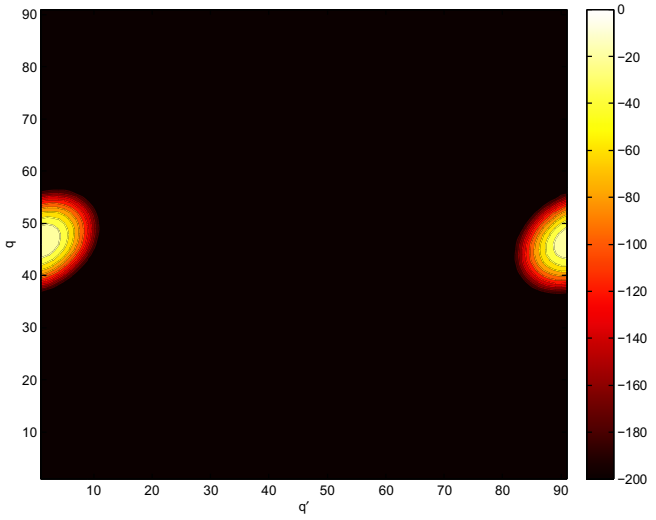

Fig. 3. Maximum and the minimum regions in the interactions of the beams of $\mathbf{T_{mm'}}$.

Fig. 4 shows the normalized magnitude of the interactions of the elements of the matrix $T_{mm'}$, which have been organized in ascending order and compared to the several threshold errors. It is possible verify an abrupt decay of such magnitude that, on its turn, is due to the natural Gaussian like windowing property of the CSBs. Hence, it is proven that only a small portion of these interactions are really relevant, making the truncation possible. This way, the interactions are reduced to $Q_t \sim \sqrt{Q}$, being Q_t the number of truncated beams used in the group interactions. In the example presented, the total number of interactions was 8281, $Q = 91$ and $Q_t \simeq 9$.

V. Conclusion

The CSB-MoM [6] appears to be potentially useful to the reduction of computational costs in the analysis of large terrain EM problems. Therefore, because the terrains are electrically large in relation to the wave length and need a large amount of segmentation, we can affirm that the CSB-MoM is more efficient than the conventional MoM. In other words, in the CSB-MoM the level of complexity is established as $O(N^{3/2})$ [3] whereas the MoM's is $O(N^2)$.

Therefore, the parameter choice must be made very carefully to avoid imprecision and spoiling the analysis. It is also important to observe another parameter choice: the number

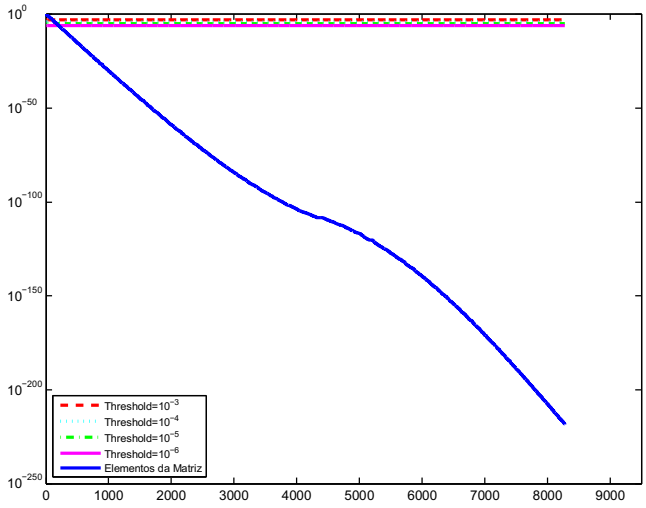

Fig. 4. The behavior of the magnitude of elements of $\mathbf{T_{mm'}}$.

of CSP beams (Q) that favors the precision of the hybrid technique corresponds to the reason between the profile segmentation (N) and the number of groups defined (M). This way, the profile geometry is directly responsible for the definition of the growth of this complexity.

Acknowledgment

This work was partially supported by CAPES, CNPq, FAPEMIG and INCTCSF.

References

[1] K. Tap, P. Pathak, and R. Burkholder, "Exact complex source point beam expansions for electromagnetic fields," *Antennas and Propagation, IEEE Transactions on*, vol. 59, no. 9, pp. 3379–3390, Sept 2011.

[2] K. Tap, "Complex source point beam expansions for some electromagnetic radiation and scattering problems," Ph.D. dissertation, Ohio State Univ., Columbus, OH, USA, 2007.

[3] K. Tap, P. Pathak, and R. Burkholder, "Fast complex source point expansion for accelerating the method of moments," in *Electromagnetics in Advanced Applications, 2007. ICEAA 2007. International Conference on*, Sept 2007, pp. 986–989.

[4] L. B. Felsen, "Complex-source-point solutions of the field equations and their relation to the propagation and scattering of gaussian beams," *Symposia Matematica, Istituto Nazionale di Alta Matematica*, vol. 18, pp. 39–56, 1976.

[5] T. Hansen and G. Kaiser, "Huygens' principle for complex spheres," *Antennas and Propagation, IEEE Transactions on*, vol. 59, no. 10, pp. 3835–3847, Oct 2011.

[6] K. Tap, P. Pathak, and R. Burkholder, "Complex source beam-moment method procedure for accelerating numerical integral equation solutions of radiation and scattering problems," *Antennas and Propagation, IEEE Transactions on*, vol. 62, no. 4, pp. 2052–2062, April 2014.

[7] T. Senior, "Impedance boundary conditions for imperfectly conducting surfaces," *Applied Scientific Research, Section B*, vol. 8, no. 1, pp. 418–436, 1960. [Online]. Available: http://dx.doi.org/10.1007/BF02920074

[8] A. Yagbasan, C. Tunc, V. Erturk, A. Altintas, and R. Mittra, "Characteristic basis function method for solving electromagnetic scattering problems over rough terrain profiles," *Antennas and Propagation, IEEE Transactions on*, vol. 58, no. 5, pp. 1579–1589, May 2010.

[9] E. Heyman and L. B. Felsen, "Gaussian beam and pulsed-beam dynamics: complex-source and complex-spectrum formulations within and beyond paraxial asymptotics," *J. Opt. Soc. Am. A*, vol. 18, no. 7, pp. 1588–1611, Jul 2001. [Online]. Available: http://josaa.osa.org/abstract.cfm?URI=josaa-18-7-1588